Supporting Information

Hu et al. 10.1073/pnas.0908858106

SI Materials and Methods

Preparation of Ink and Films Based on CNTs. To form an ink, CNTs grown by laser ablation and SDBS (Sigma–Aldrich) were dispersed in deionized water. Their concentrations were 10 and 1–5 mg/mL, respectively. After bath sonication for 5 min, the CNT dispersion was probe-sonicated for 30 min at 200 W (VC 505; Sonics) to form an ink. Meyer rods (Rdspecialties) were used to coat the CNT ink onto Xerox paper. The sheet resistance of conductive paper was measured by using the four-point probe technique (EDTM).

Silver Nanowire Ink. Ag NWs were produced in solution-phase following the method by Xia and colleagues (1). Table S1 shows a detailed recipe for the silver nanowire synthesis, including the function of each step. In the first step, a mixture of 0.668 g of PVP and 20 mL of EG was heated in a flask at 170 °C. Once the temperature was stabilized, 0.050 g of silver chloride (AgCl) was ground finely and added to the flask for initial nucleation. After 3 minutes, 0.22 g of silver nitrate ($AgNO_3$) was titrated for 10 minutes. Then, the flask was kept at the same temperature for another 30 minutes. After the reaction was completed, the solution was cooled down and centrifuged three times to remove solvent, PVP, and other impurities.

Conformal Coating of CNTs on Xerox Paper. Figs. S1 and S2 show fiber structures of Xerox paper and the conformal coating of CNTs, respectively. The height of the fibers was about 10 μm. The fibers interpenetrated each other and made the surface of the paper rough. In Fig. S2, the conformal coating is observed in corners, holes, and edges of all fibers in paper. The fibers in paper formed microscale pores, and the coated CNTs formed nanoscale pores.

Properties of Conductive Paper. We performed a washing test on the CNT films on paper to demonstrate the strong binding between the CNTs and paper. The conductive CNT paper made from nonwoven polyester/cellulose paper from Berkshire went through various testing procedures in water, such as soaking, rinsing, and squeezing. After these tests, the conductive paper was dried at 80 °C for 10 min. The resistance was measured before and after these tests, and no obvious resistance change was observed.

As described in the main text, the sheet resistance was measured before and after the washing process for both paper and PET. Local resistance is presented alongside global resistance in Fig. S3*A*. The local resistance refers to that within a piece of continuous film with size around a few millimeters, and the global resistance indicates that over many pieces of such local films.

Various Coating Methods. For Meyer rod coating of CNT films, CNT ink was dropped onto the paper surface. Then, the rod was rolled to the other end of the paper. The thickness of the dried CNT film could be controlled by the ink concentration and the wire size of the Meyer rods. To write with Chinese calligraphy, nonwoven polyester/cellulose paper (DURX 670; Berkshire) was used to achieve enough absorption of ink into the paper. Also, to realize direct writing with CNT ink, a highlighter pen was disassembled, and the original ink was replaced with CNT ink. The writing of CNT ink using the highlighter pen is shown in Fig. S3*B*. The paper substrate absorbed the CNT ink easily, whereas flat solid substrates, such as PET, did not absorb the ink at all. The resistance of such directly written CNT patterns using the pen is around 300 Ω/sq for paper and around 1 MΩ/sq for PET.

CNT–Ag NW Interface and Contact Resistance. We also tested Ag NW coatings on top of CNT films, where Ag NWs can be used as global current collectors and CNTs as local current collectors for large-scale energy-storage devices. The effective thicknesses of the CNT and Ag NW films were 160 and 400 nm, respectively. Fig. S4*D Inset* shows a scheme for measuring the contact resistance between CNTs and Ag NWs. The width of the CNT film was 6 mm. The R_s for CNTs and Ag NWs were 92 and 2 Ω/sq, respectively. Ag NW films with 1.5 mm in width and 6 mm in length were coated on top of CNT films. The contact resistance, extracted from the linear fit in the graph of resistance vs. distance between Ag NW electrodes (Fig. S4*D*), was 0.83 Ω for 0.09 cm^2, which corresponds to a specific contact resistance of 0.075 Ω·cm^2 for this measurement configuration. Consequently, the contact resistance is negligible compared with the sheet resistance of Ag NW film, and thus is not a limiting factor in charge transfer.

SC Cell Preparation. For aqueous electrolyte devices, two pieces of CNT conductive paper were first attached on glass slides. CNT films were used as both electrodes and current collectors. At the end of the CNT paper, a small piece of platinum was clipped onto the CNT conductive paper by a toothless alligator clip to connect to a battery analyzer (Maccor 4300). Both glass slides were assembled with a separator (Whatman 8-μm filter paper) sandwiched in between. The paper assembly was wrapped with parafilm and then dipped in the electrolyte solution. The active area overlapped by both CNT conductive papers was 1 cm^2.

For organic electrolyte devices, cells were assembled by inserting the same separator soaked with the standard battery electrolyte (1 M $LiPF_6$ in ethylene carbonate:diethylene carbonate = 1:1 vol/vol; Ferro) between two CNT conductive paper substrates. The active area overlapped by both CNT conductive paper substrates was also 1 cm^2. Then, the entire assembly was sealed in a polybag (Sigma–Aldrich). As in the aqueous cells, small pieces of platinum were attached to the end of CNT conductive paper for a good electrical contact. The current collectors came out through the sealed edges of polybags and then were connected to the battery analyzer. All steps in the cell preparation were done in an argon filled glove box (oxygen and water contents below 1 and 0.1 ppm, respectively).

Typical mass loadings for data shown in Fig. 3 *C* and *D* are 72 ≈ 270 μg/cm^2. Larger mass loadings up to 1.7 mg/cm^2 were also tested, and the capacitances are plotted in Fig. S6.

Measurements. Capacitance, energy density, and power density are all characterized by galvanostatic measurements. A total of 0.02 ≈ 20 mA/cm^2 was applied to cells while potentials between both electrodes swept between cutoff values ($0 \le V \le 0.85 \approx 1$ V in aqueous phase, $0 \le V \le 2.3 \approx 3$ V in organic phase). Voltages were recorded every 0.01 ≈ 0.2 seconds. For the cycling test in both phases of electrolyte, ≈5 A/g was applied. The cutoff potentials for the sulfuric acid and organic electrolyte were 0.85 and 2.3 V, respectively.

Data Analysis. In the galvanostatic data, the IR drop at the upper cutoff potential and slope in the discharge curve were used to obtain the power and energy densities, respectively. The power was calculated by using

$$P = V^2/[4RM]$$

where V is the cutoff potential, R is the internal resistance, and M is the total mass of CNTs on both sides. The internal resistance

was evaluated from the voltage drop at the beginning of each discharge:

$$R = \Delta V_{iR}/2i$$

ΔV_{iR} is the voltage drop between the first two points in the voltage drop at its top cutoff. This voltage drop is also referred to as *iR* drop. i is the current applied.

The specific capacitance (C_s) was calculated by using

$$C_s = i/-[\Delta V/\Delta t]m = i/-(\text{slope}\cdot m)$$

where i is the current applied, the slope is that of the discharge curve after the *iR* drop, and m is the mass of CNTs on one electrode. Similarly, energy density (E) was calculated using

$$E = 0.5CV^2/M$$

where V and M are the same notations as the power calculation, and C is the measured capacitance. All of the calculations here are consistent with those described elsewhere (2).

CV Data. CV data in both electrolytes are presented in Fig. S5.

SC Performance. CNT conductive paper with different CNT film thicknesses were prepared and tested (Fig. S6*A*). As expected, the capacitance per area increased with film thickness. Data from CNT paper with different mass loadings are presented in Fig. S6*B*. The device with 1.33 mg/cm^2 showed larger gravimetric capacitances than those of PET device with ≈20 times lower mass loading. This indicates that the advantages of paper, such as strong binding of CNTs and easy ion accessibility, are still valid for thicker films.

Areal capacitance was measured for the CNT conductive paper measured in organic and aqueous electrolytes with mass loading of 1.7 and 1.33 mg/cm^2, respectively (Fig. S6*C*). These values were compared with reported data from the highest-density CNT assembly (3) in figure 4*C* of ref. 3. Volumetric capacitances of the CNT assembly were converted to areal capacitances considering the assembly length (100 μm). Even if our film thickness (≈13.3 μm) was about 10 times smaller than that of the highly dense CNT assembly, our conductive paper showed larger areal capacitance at all current values. The excellent capacitance of the conductive paper confirms the superior ionic accessibility for SC operations.

Battery Fabrication and Test. The cathode materials $LiMn_2O_4$ nanorods were synthesized according to previous work (4). Typically, 8 mmol $MnSO_4{\cdot}H_2O$ and 8 mmol $(NH_4)_2S_2O_8$ were dissolved in 20 mL of deionized water, and the solution was transferred to a 45-mL, Teflon-lined stainless steel vessel (Parr). The vessel was sealed and heated at 150 °C for 12 h to obtain β-MnO_2 nanorods. The as-synthesized MnO_2 nanorods are mixed and ground with lithium acetate (Aldrich) at a molar ratio of 2:1. One milliliter of methanol was added to make a uniform slurry mixture. Then, the mixture was sintered at 700 °C for 10 h under air to obtain $LiMn_2O_4$ nanorods. $Li_4Ti_5O_{12}$ powder was used as received from Süd Chemie.

Electrodes for electrochemical studies were prepared by making slurry of 70 wt % active materials, 20 wt % Super P Carbon, and 10 wt % PVDF binder in NMP as the solvent. The slurry was coated onto a piece of conductive CNT paper by an applicator and then dried at 100 °C in an vacuum oven overnight.

The half-cell tests of both cathode ($LiMn_2O_4$) and anode ($Li_4Ti_5O_{12}$) were carried out inside a coffee bag (pouch) cell assembled in an argon-filled glovebox (oxygen and water contents below 1 and 0.1 ppm, respectively). Lithium metal foil (Alfa Aesar) was used as the counter electrode in each case. A 1 M solution of $LiPF_6$ in EC/DEC (1:1 vol/vol, Ferro) was used as the electrolyte, with separators from Asahi Kasei. The charge/discharge cycles were performed at different rates at room temperature, where 1C was 148 mA/g for $LiMn_2O_4$ and 175 mA/g for $Li_4Ti_5O_{12}$, respectively. The voltage range was 3.5–4.3 V for $LiMn_2O_4$ and 1.3–1.7 V for $Li_4Ti_5O_{12}$. Tests were performed by either Bio-Logic VMP3 battery testers or MTI battery analyzers.

The fabrication of full cells was slightly different. To achieve the high voltage to light a blue LED, silicon/carbon core shell nanowires were used as anode. The core shell nanowires were synthesized by CVD method. Carbon nanofibers (Sigma–Aldrich) were loaded into a tube furnace and heated to 500 °C. Then, silane gas was introduced and decomposed onto carbon nanofibers. The weight ratio of silicon shell to carbon core was typically ≈2:1. As-synthesized Si/C nanowires were dropped onto a CNT paper to form an anode. After this step, cathode ($LiMn_2O_4$) and anode (Si/C nanowires) films were assembled to make a 5 cm^2 pouch cell as described above, and it was used to repeatedly light the blue LED.

Resistance Issue for Practical Batteries. The figure above is a scheme of the rectangular electrode in real cylindrical batteries (5). In cylindrical batteries, current flows along the long side of the rectangular electrode film. However, as shown in Fig. S7, by adding a highly conductive strip parallel to the long side in the middle of an electrode film, current can flow to the metal strip first and then to the lead. This highly conductive strip could be either a thin metal foil or Ag NW paint, as mentioned in the main text. As a result, the resistance in such configuration is much smaller than the sheet resistance of conductive paper. In an 18650 cylindrical cell, the typical size of an electrode is 5 × 50 cm (5). In this paper, 20 Ω/sq conductive paper was used as the current collector, so the resistance of each half-electrode film was 20 Ω/sq ÷ (50 cm/2.5 cm) ÷ 2 = 0.5 Ω. The factor of 2 comes from the fact that current was generated uniformly through the whole electrode. Because the two half-electrode films were in parallel, the total resistance of a single electrode could further decrease to 0.5 Ω ÷ 2 = 250 mΩ, which is within the same order of magnitude of commercial Li-ion batteries (50–100 mΩ). Moreover, because the process of making paper current collector has not been optimized, we believe that 1 Ω/sq CNT paper could be realized through the following methods: optimization of coating process, moderate increase of CNT loading, selective use of metallic CNTs, and mixing with metal nanowires. Consequently, the total resistance of two paper electrodes is 12.5 mΩ * 2 = 25 mΩ, which is much smaller than the internal resistance in practical Li-ion batteries. In a word, the resistance concern for CNT conductive paper is resoluble by combination of various methods.

Gravimetric Energy Density of Conductive Paper Batteries Compared with Commercial Batteries. In typical Li-ion batteries, the capacity density is 3–5 mAh/cm^2, which corresponds to 21–36 mg/cm^2 $LiCoO_2$ (140 mAh/g) and 10–17 mg/cm^2 graphite (300 mAh/g). The current collector includes 20≈25 μm Al foil (2.7 g/cm^3) and 10–20 μm Cu foil (9.0 g/cm^3). The total weight of electrodes (electrode materials and current collectors in both sides) counts for ≈60% of the total weight of a battery (5). In contrast, the density of paper is ≈1.0 g/cm^3 and the loading of CNTs is 0.2 mg/cm^2 for a sheet resistance of 20 Ω/sq. The lower density of CNT conductive paper leads to higher gravimetric energy density. Table S2 shows the comparison of the weight of commercial batteries and conductive paper batteries. The thickness of paper is assumed to be the same as that of metal current collectors. In this table, "commercial" refers to commercial Li-ion batteries, and "paper" means conductive paper batteries discussed in this paper. The weight saved could be close to 20%. The unit for all numbers in the table is milligrams.

1. Sun YG, Mayers B, Herricks T, Xia YN (2003) Polyol synthesis of uniform silver nanowires: A plausible growth mechanism and the supporting evidence. *Nano Lett* 3:955–960.
2. Frackowiak E (2007) Carbon materials for supercapacitor application. *Phys Chem Chem Phys* 9:1774–1785.
3. Futaba DN, et al. (2006) Shape-engineerable and highly densely packed single-walled carbon nanotubes and their application as super-capacitor electrodes. *Nat Mater* 5:987–994.
4. Kim DK, et al. (2008) Spinel LiMn2O4 nanorods as lithium ion battery cathodes. *Nano Lett* 8:3948–3952.
5. Johnson BA, White RE (1998) Characterization of commercially available lithium-ion batteries. *J Power Sources* 70:48–54.

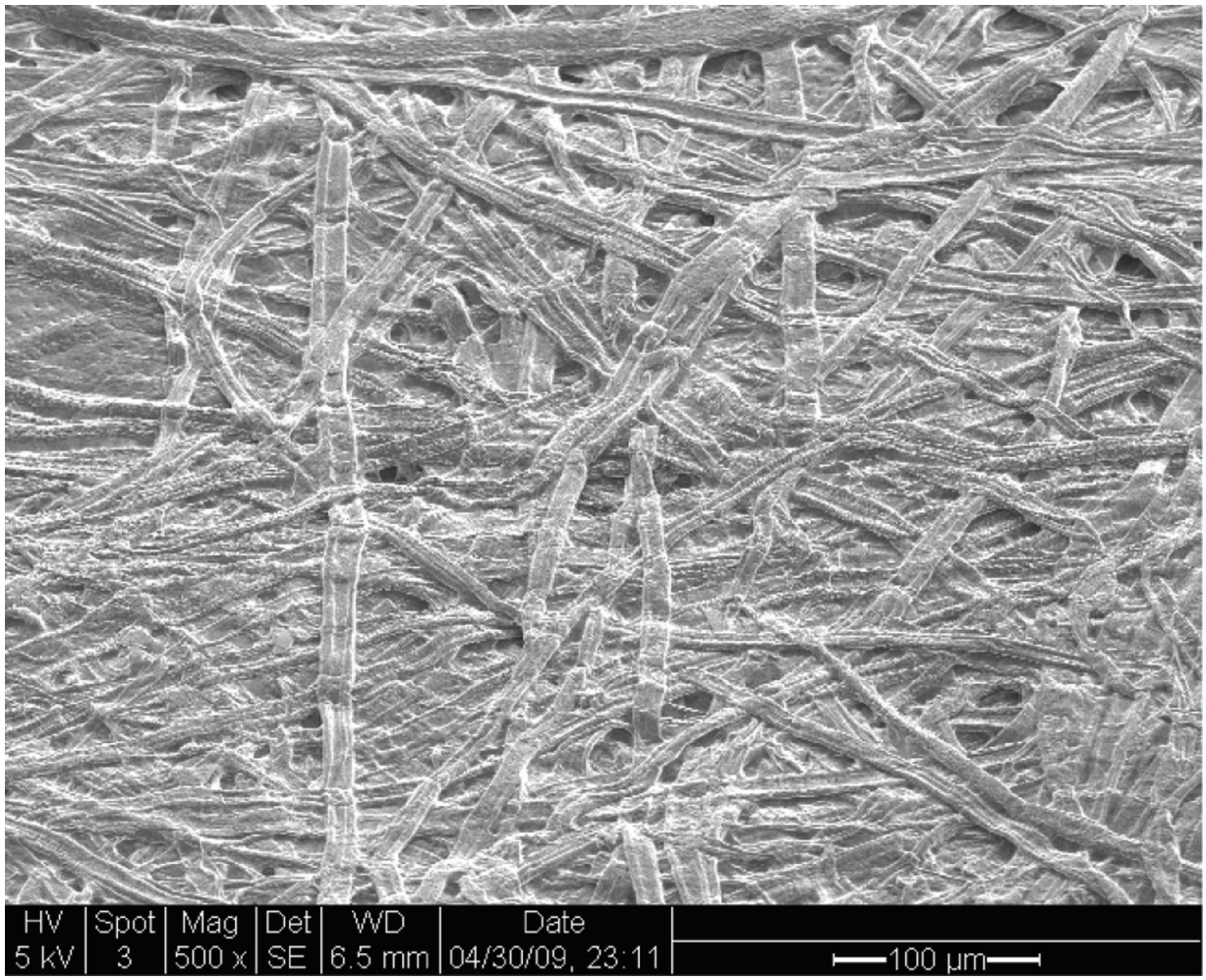

Fig. S1. The SEM image showing the fiber structures of Xerox paper.

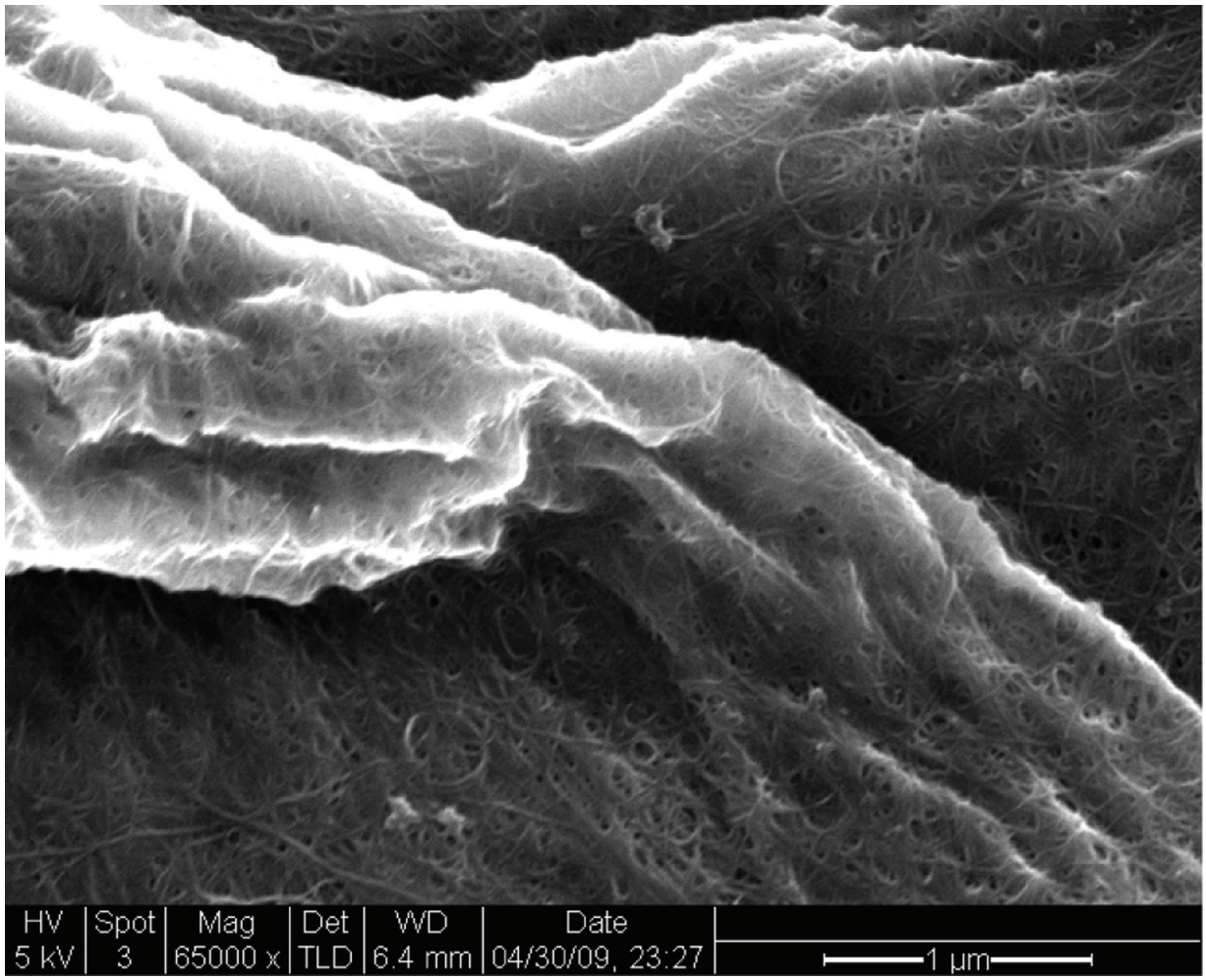

Fig. S2. The high-resolution SEM image showing the conformal coating of CNTs on Xerox paper surface.

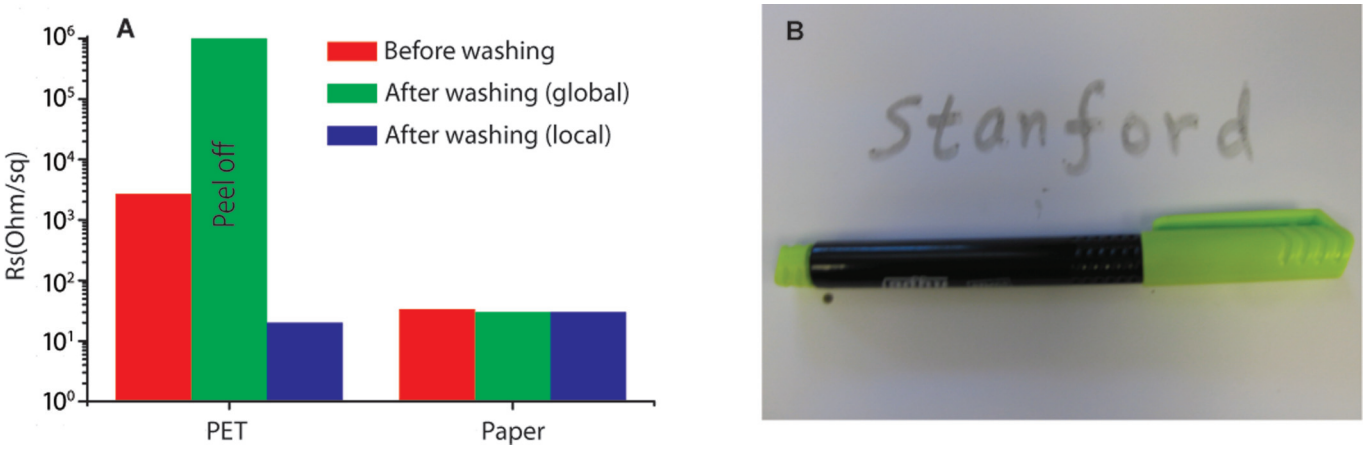

Fig. S3. Properties of CNT films. (*A*) The global and local sheet resistances for PET and paper before and after the surfactant washing process. The error ranges of all of the bars presented here and in Fig. 2*A* are ±10%. (*B*) The writing of CNT ink by using a highlighter pen.

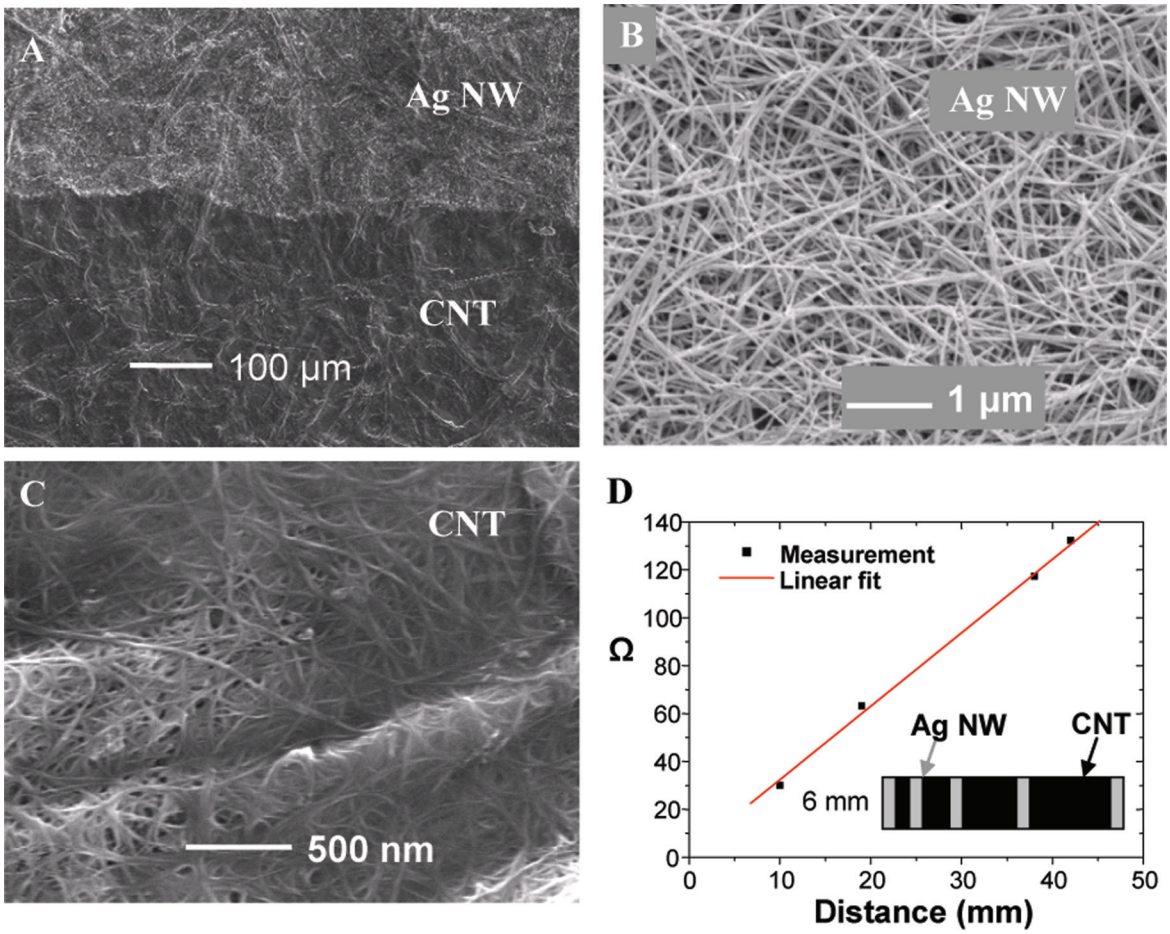

Fig. S4. SEM images of (*A*) interface between CNTs and Ag NWs on Xerox paper, (*B*) Ag NW film, and (*C*) CNT film. (*D*) The resistance scaling with the Ag NW electrode distance. (*Inset*) Contact resistance measurement scheme.

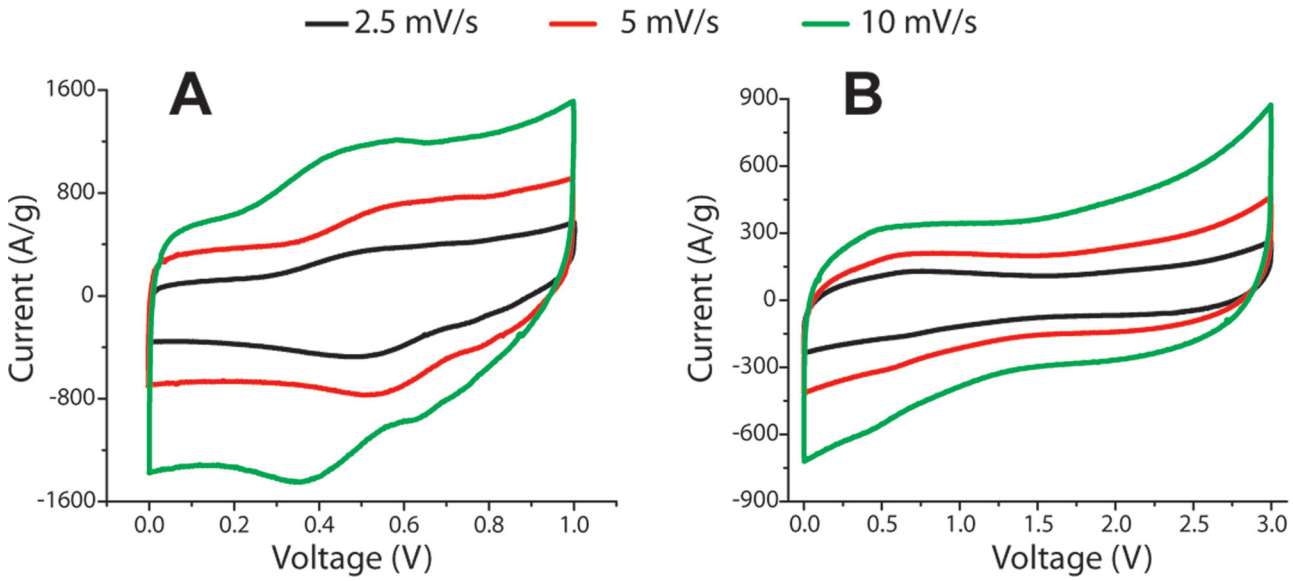

Fig. S5. CV data measured at different sweep rates in (*A*) 1 M sulfuric acid and (*B*) organic electrolyte (1 M $LiPF_6$ in ethylene carbonate:diethylene carbonate = 1:1 vol/vol).

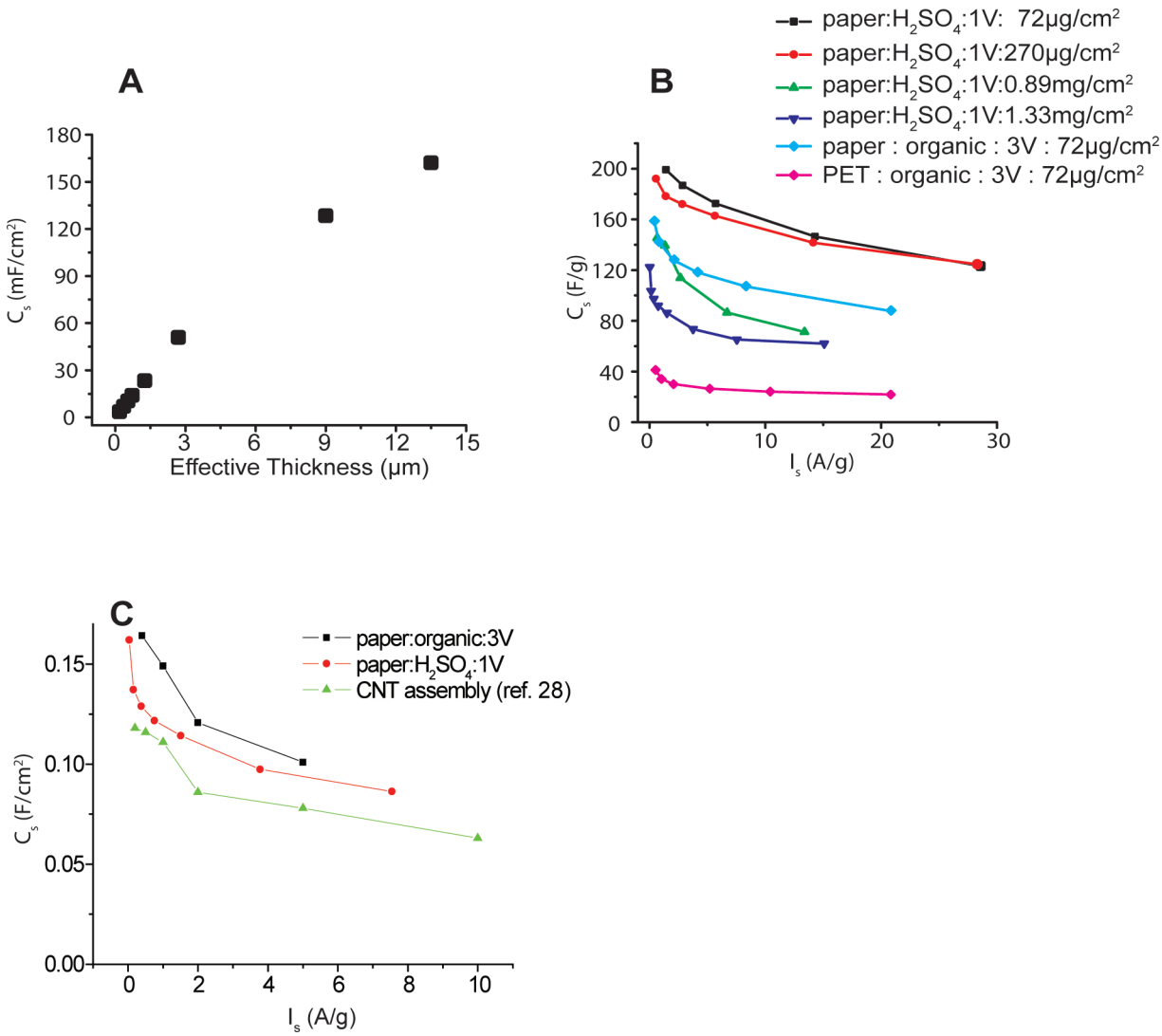

Fig. S6. Performance of CNT on paper as supercapacitors. (*A*) Thickness dependence of specific capacitance per area. The samples are measured in 1 M sulfuric acid and 1-V range. (*B*) Mass loading dependence of gravimetric capacitance. The PET device with the lowest mass loading is plotted together for comparison. (*C*) Areal capacitance at various currents. Mass loadings for organic and aqueous electrolytes are 1.33 and 1.7 mg/cm^2, respectively. Highly dense CNT solid data from Futaba et al. (1) is plotted together for comparison. Their CNT solids are ≈100 μm thick, which is about 10 times thicker than our film. The data in *B* and *C* are calculated based on CNTs mass only.

1. Futaba DN, et al. (2006) Shape-engineerable and highly densely packed single-walled carbon nanotubes and their application as super-capacitor electrodes. *Nat Mater* 5:987–994.

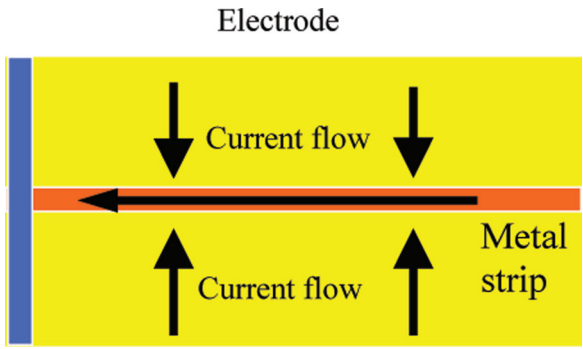

Fig. S7. Design of adding metal strip at the long side of the rectangular film to decrease the resistance of current collectors. The blue line on left is the metal lead used in commercial batteries.

Table S1. The step-by-step standard recipe for Ag NW synthesis

Step	Details	Condition	Time	Function
1	0.668 g of PVP plus 20 mL EG	170 °C	20≈30 min	Stabilizing temperature
2	0.050 g of AgCl, finely ground	170 °C	3 min	Seed formation
3	0.220 g of $AgNo_3$ plus 10 mL of EG	170 °C	10 min	Growing nanowires
4	Cooking	170 °C	30 min	Completing growth
5	Centrifuge with methanol	4991 × *g*	30 min	Remove EG, PVP, ions

Table S2. Comparison of the weight between commercial batteries and conductive paper batteries

	3 mAh/cm^2		5 mAh/cm^2	
Capacity loading	Commercial	Paper	Commercial	Paper
Cathode ($LiCoO_2$)	21	21	36	36
Cathode collector/20 μm	5.4	2.2	5.4	2.2
Anode (graphite)	10	10	17	17
Anode collector/15 μm	13.4	1.7	13.4	1.7
Other components*	33.2	33.2	47.9	47.9
Total weight	83	68.1	119.7	104.8
Weight saved, %		18.0		12.4

*The weight of other components (electrolyte, separators, can) is supposed to be 40% of the total weight of a battery, which is the same as two-thirds of the weight of both electrodes (electrode materials and current collectors in both sides). Weights are in milligrams.